BIOCHEMISTRY
including biophysical chemistry & molecular biology

Article

pubs.acs.org/biochemistry

Lipid Bilayer Properties Control Membrane Partitioning, Binding, and Transport of P-Glycoprotein Substrates

Adam T. Clay and Frances J. Sharom*

Department of Molecular and Cellular Biology and Biophysics Interdepartmental Group, University of Guelph, Guelph, Ontario, Canada N1G 2W1

Supporting Information

ABSTRACT: The ABC protein P-glycoprotein (Pgp or ABCB1) is a multidrug efflux pump capable of transporting many structurally diverse substrates from within the lipid bilayer. Previous studies have demonstrated the importance of the membrane in modulating Pgp function, but few have quantified these effects. We employed purified Pgp reconstituted into phospholipid bilayers with defined gel to liquid-crystalline melting transitions to investigate the effect of membrane environment on the transporter and three of its substrates. Equilibrium dialysis measurements indicated that Hoechst 33342, LDS-751, and MK-571 partitioned much more readily into liquid-crystalline phase bilayers than into gel phase bilayers. However, drug binding affinities revealed that Pgp bound the three substrates more tightly when the lipid bilayer was in the gel phase. The binding affinity of the transporter for substrates within the bilayer was low, in the millimolar range, suggesting that it interacts with them weakly. Thermodynamic analysis revealed that both drug-Pgp and drug-lipid interactions contribute to binding affinity. The kinetics of LDS-751 and Hoechst 33342 transport by reconstituted Pgp was monitored using a real-time fluorescence-based assay to obtain apparent turnover frequencies. Transport rates were found to be sensitive to both drug structure and lipid environment. Arrhenius and transition state analysis of transport rates suggested that the rate of drug transport depends on both the affinity of Pgp for substrate and protein conformational changes. Transport rates did not appear to be limited exclusively by the rate of ATP hydrolysis and may be partially controlled by the rate of drug dissociation.

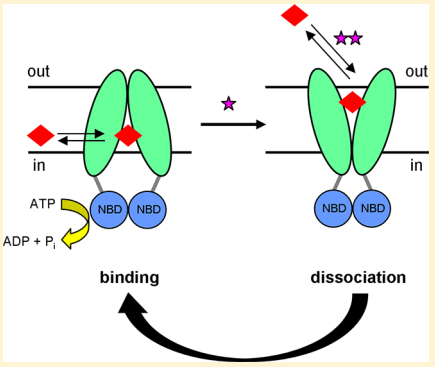

Most members of the ubiquitous ATP-binding cassette (ABC) superfamily are pumps that couple ATP hydrolysis to the active transport of substrates across membranes.[1] One of the best characterized ABC proteins is P-glycoprotein (Pgp or ABCB1), an ~170 kDa mammalian glycoprotein that functions as a polyspecific multidrug efflux pump.[2−4] Overexpression of Pgp in the plasma membrane of tumor cells contributes to multidrug resistance (MDR) of human cancers to chemotherapeutic drugs, a serious problem in clinical therapy.[3,5,6] In accordance with the common architecture shared by ABC proteins,[7] Pgp comprises two transmembrane domains and two cytosolic nucleotide binding domains (NBDs) that bind and hydrolyze ATP.

Pgp substrates are typically amphipathic, and there is considerable evidence that the protein binds its substrates from within the membrane and transports them to either the extracellular milieu or the opposing membrane leaflet.[3,5] Indeed, the protein has been shown to function as a flippase for various fluorescent lipid analogues in reconstituted proteoliposomes.[8,9] The putative drug transport route in the X-ray crystal structure of *Caenorhabditis elegans* Pgp is open to the cytoplasmic side of the membrane, suggesting that drugs can enter the pocket from the inner membrane leaflet.[10] This intimate connection with the membrane suggests that the transporter may be profoundly affected by the physicochemical properties of the host bilayer. Indeed, membrane composition and biophysical properties are known to affect Pgp function. For example, Pgp ATPase activity is modulated by both membrane lipids and detergents.[11−13] The binding affinity of reconstituted Pgp for drug substrates is sensitive to phospholipid headgroup, acyl chain length, and lipid fluidity.[14] In proteoliposomes, the rate of transport of tetramethylrosamine, a high-affinity Pgp substrate, was found to be relatively high in the gel phase, maximal near the gel to liquid-crystalline transition temperature, T_m, and lowest in the liquid-crystalline phase.[15] In contrast, Pgp had a higher ATP binding affinity and higher values of K_M, V_{max}, and activation energy for ATP hydrolysis in liquid-crystalline bilayers than in gel phase bilayers.[16] Inclusion of cholesterol in the host bilayers was also found to affect drug binding, drug transport, and ATPase activity.[17] Finally, a decrease in the lateral packing density of the bilayer has been proposed to influence the thermodynamics of ATP hydrolysis.[18] Thus, the membrane phase state, composition, and fluidity appear to be important parameters in the ability of Pgp to bind and transport drugs. However, the means by which membrane properties affect Pgp function are not fully understood.

Received: November 13, 2012
Revised: December 24, 2012
Published: December 26, 2012

The drug transport mechanism of Pgp remains controversial,[19,20] but crystal structures determined for mouse[21] and *C. elegans*[10] Pgp and other ABC transporters[7,22] have provided structural information about several aspects of substrate binding, transport, and ATP hydrolysis. It is generally believed that Pgp exists in at least two major conformations during the catalytic cycle, an "inward-facing" conformation with the high-affinity drug binding pocket exposed to the cytoplasmic leaflet of the membrane and an "outward-facing" conformation in which the drug binding site has a lower affinity and is exposed to the outer leaflet or extracellular space. Conversion of the inward-facing conformation to the outward-facing conformation requires hydrolysis of ATP, whereas subsequent nucleotide exchange and/or product release involving one (or both) NBD(s) is presumed to reset the transporter to the transport-competent inward-facing conformation.[23]

The development of agents that can effectively inhibit Pgp-mediated MDR has been an important and long-standing goal in anticancer therapy.[24,25] Early work showed that Pgp transport function in plasma membrane vesicles and intact cells could be altered by changes in membrane fluidity induced by small molecule fluidizers, surfactants, and amphiphiles.[26−28] The mechanism of MDR reversal in this case does not appear to involve direct interaction between these agents and Pgp and may be linked to increases in membrane permeability.[29] From these studies, it has been proposed that changing the properties of the membrane may be a useful approach for clinical MDR reversal.[30] If such a strategy is to be successful, it is clearly important to have a good understanding of how the properties of the lipid environment affect all aspects of the Pgp catalytic cycle.

In this work, purified Pgp was reconstituted into host phospholipid bilayers of well-defined composition. The phospholipids, 1,2-dimyristoylphosphatidylcholine (DMPC) and 1-palmitoyl-2-myristoylphosphatidylcholine (PMPC), were chosen as host lipids because they undergo a gel to liquid-crystalline phase transition at a well-defined melting temperature, T_m (T_m values of ∼23 and ∼28 °C for DMPC and PMPC, respectively). Three structurally diverse compounds were used as Pgp transport substrates. Via analysis of the temperature dependence of their lipid−water partition coefficients, binding affinities, and transport rates above and below the T_m of the bilayer, insight was gained into how the membrane modulates drug binding and transport by Pgp.

MATERIALS AND METHODS

Materials. 3-[(3-Cholamidopropyl)dimethylammonio]-1-propanesulfonate (CHAPS) was obtained from MP Biomedicals (Solon, OH). Hoechst 33342 (H33342) and 2-{4-[4-(dimethylamino)phenyl]-l,3-butadienyl}-3-ethylbenzothiazolium perchlorate (LDS-751) were purchased from Invitrogen (Burlington, ON). ATP, *N*-acetyl-tryptophanamide (NATA), 5-{3-[2-(7-chloroquinolin-2-yl)ethenyl]phenyl}-8-dimethylcarbamyl-4,6-dithiaoctanoic acid sodium salt hydrate (MK-571), and *o*-vanadate were purchased from Sigma-Aldrich Canada (Oakville, ON). Phospholipids were acquired from Avanti Polar Lipids (Alabaster, AL). α-Minimal essential medium was purchased from Invitrogen. All other cell culture supplies were obtained from HyClone Laboratories (Logan, UT).

Pgp Purification and Reconstitution. Plasma membrane vesicles were isolated from CH_RB30 cells as previously described.[31] Pgp was purified from the vesicles using a modified version of an established protocol,[17,32] by initial extraction with 15 mM CHAPS in HEPES buffer [20 mM HEPES, 100 mM NaCl, and 5 mM $MgCl_2$ (pH 7.4)]. Solubilization of the pellet in HEPES buffer containing 45 mM CHAPS yielded partially purified Pgp, which was further purified using affinity chromatography by two passes through a concanavalin A-Sepharose column pre-equilibrated with HEPES buffer containing 2 mM CHAPS. A colorimetric assay was used to determine ATPase activity as described previously.[33] Purified Pgp had high ATPase activity (1.6−2.2 μmol min^{-1} mg^{-1}) and a protein concentration of >350 μg/mL.

Reconstitution of Pgp into proteoliposomes was conducted using gel filtration chromatography as described previously.[8] The final lipid:protein ratio of the proteoliposomes was 2.5−3:1 (w/w), as determined using a phosphatidylcholine (PC) assay kit (Cayman Chemical, Ann Arbor, MI) and Bradford protein assay.[34] Where needed, the lipid volume was estimated from the phospholipid concentration assuming densities of 1.03 g/mL for the liquid-crystalline phase phospholipid and 1.06 g/mL for the gel phase phospholipid.[35] A CHAPS assay[36] was used to verify that the proteoliposomes contained undetectable levels of detergent.

Lipid−Water Partitioning of Drugs. Apparent lipid−water partition coefficients (K_{lip}) were determined for LDS-751, H33342, and MK-571 in DMPC and PMPC vesicles at several temperatures spanning their T_m values, using an equilibrium dialysis method,[37] with minor modifications. Vesicles were prepared by suspending 1 mg of dried phospholipid in 1 mL of HEPES buffer by vigorous vortexing and extrusion through a 100 nm polycarbonate filter. A 600 μL aliquot of vesicles was placed in dialysis tubing (12−14 kDa molecular mass cutoff) and dialyzed against 100 mL of HEPES buffer containing 3.5 μM LDS-751, 7.0 μM H33342, or 3.5 μM MK-571. After 24 h in a controlled temperature shaker at the desired temperature, 150 μL aliquots of dialysis buffer and the lipid sample inside the dialysis tubing were removed and placed in a 96-well microplate; 150 μL of 10 mM SDS in HEPES buffer was added to each well, and the plate was incubated at room temperature for 10 min. The concentration of the drug in the aqueous and lipid samples was determined using fluorescence spectroscopy ($\lambda_{ex,LDS\text{-}751}$ = 544 nm, $\lambda_{em,LDS\text{-}751}$ = 710 nm, $\lambda_{ex,H33342}$ = 355 nm, $\lambda_{em,H33342}$ = 460 nm, $\lambda_{ex,MK\text{-}571}$ = 355 nm, and $\lambda_{em,MK\text{-}571}$ = 405 nm, with 10 nm slit widths) by comparison to a standard curve for each drug (0−3.5 μM), using a fluorescence plate reader. K_{lip} was calculated from the relative drug concentrations in the lipid and buffer compartments, as described previously.[37] Where needed, the lipid volume was estimated from the phospholipid concentration, assuming densities of 1.03 g/mL for the liquid-crystalline phase phospholipid and 1.06 g/mL for the gel phase phospholipid.[35]

Pgp Substrate Binding Affinity. The Pgp binding affinity for LDS-751, H33342, and MK-571 was determined by quenching of the intrinsic Trp fluorescence of the purified protein in either a 2 mM CHAPS solution or proteoliposomes, as described previously.[17,32] Fluorescence was monitored using a PTI QuantaMaster C-61 or QM-8 steady state fluorimeter (Photon Technology International, London, ON), with excitation at 290 nm (2 nm slit width) and emission at 330 nm (6 nm slit width). Curves were baseline-corrected for nonspecific quenching and inner filter effects by performing an identical titration using the soluble Trp analogue, NATA. Experiments were performed at several temperatures spanning the T_m values for each phospholipid bilayer. No statistical differences were observed for NATA quenching at the different

temperatures used in these studies, so NATA quenching data obtained at one temperature were used to correct all temperatures. Quenching of Trp fluorescence at each drug concentration was fit to the following equation using SigmaPlot (Systat, Chicago, IL)

$$\frac{\Delta F}{F_0} \times 100 = \frac{(\Delta F_{max}/F_0) \times 100[D]}{K_d + [D]} \quad (1)$$

where $\Delta F/F_0 \times 100$ represents the percent change in fluorescence intensity relative to the initial value after addition of drug at concentration [D] and $\Delta F_{max}/F_0 \times 100$ is the maximal percent fluorescence quenching. K_d(app) represents the apparent affinity of Pgp for the substrate from the aqueous phase. Because Pgp actually binds its substrates from the lipid phase, the affinity of Pgp for the substrate from within the lipid bilayer, K_{dlip}, was calculated using[38]

$$K_{dlip} = \frac{K_d}{\frac{V_{lip}}{V} + \frac{1}{K_{lip}}} \quad (2)$$

where V is the total volume of the sample and V_{lip} is the volume of lipid in the sample.

LDS-751 and H33342 Transport Kinetics. Initial rates of Pgp-mediated LDS-751 and H33342 transport were determined using a modified version of an established real-time fluorescence-based assay;[15,17] 100 μL of HEPES buffer and 100 μL of Pgp proteoliposome sample containing the desired drug concentration (4 μM LDS-751 or 5 μM H33342 for phase transition studies) were mixed and incubated at the desired temperature for 10 min in a temperature-controlled water bath and then added to a thermostated 0.5 cm × 0.5 cm quartz cuvette. The drug was excited (for LDS-751, λ_{ex} = 555 nm, with a 2 nm slit width; for H33342, λ_{ex} = 355 nm, with a 2 nm slit width), and its emission was monitored continuously (for LDS-751, λ_{em} = 688 nm, with a 6 nm slit width; for H33342, λ_{em} = 450 nm, with a 2 nm slit width) for 150 s. At this time, 50 μL of temperature-equilibrated ATP with a regenerating system (25 mM ATP, 11.5 mg/mL creatine phosphate, and 0.3 mg/mL creatine kinase in HEPES buffer) was added to initiate transport, and the fluorescence emission was monitored for an additional 210 s. Less than 2% of the total fluorescence signal arose from aqueous drug (data not shown); therefore, it was assumed that lipid-bound drug was responsible for all observed fluorescence. The fluorescence data were converted into concentration using

$$[D]_i = [D]_{o,aq} K_{lip} \frac{F_i}{F_0} \quad (3)$$

where $[D]_i$ is the concentration of drug in the membrane at time i, $[D]_{o,aq}$ is the initial aqueous concentration of drug, K_{lip} is the lipid−buffer partition coefficient at the appropriate temperature, and F_i/F_0 is the fractional fluorescence at time i relative to the fluorescence at the time of ATP addition. As a control to verify that fluorescence changes were caused by Pgp transport, and not by dynamic repartitioning of the drug as a result of dilution, 100 μM o-vanadate was added to a subset of samples at the same time as the drug. Initial transport rates (micromolar per second) were determined by taking the slope of the linear section from 10 to 20 s following the addition of ATP, after subtraction of the vanadate control. These rates were converted to apparent turnover frequencies, k_{app}, by accounting for membrane volume and drug concentration and assuming a molecular mass for Pgp of 170 kDa, as described in section S1 of the Supporting Information.

For technical reasons, it was not possible to perform transport experiments at close to saturating drug concentrations. The estimated rate constants should not be interpreted as absolute rate constants, as they do not represent the intrinsic (saturated) rate constants. Further, the reaction rates appear to be controlled, in part, by the rate of dissociation of the drug from the transition state (see later), which complicates their interpretation. Apparent rate constants, and the apparent transition state thermodynamic parameters derived from them, are valid for the substrate concentrations used in the assays.

Temperature Dependence of Equilibrium and Kinetic Rate Constants. van't Hoff analysis of equilibrium constants (K_{lip}, K_d, and K_{dlip}) was performed to obtain the $\Delta H°$ and $\Delta S°$ parameters for each process (see section S2 of the Supporting Information). Lipid-independent thermodynamic changes occurring during the formation of the drug−protein complex in two different lipid environments were assessed by comparing the ΔH^{rel}_{dp} or ΔS^{rel}_{dp} parameters; a difference in the values of ΔH^{rel}_{dp} or ΔS^{rel}_{dp} for the same drug in two different lipid environments was interpreted as a lipid-independent change in the thermodynamics of formation of the Pgp−drug complex. These parameters allow for a relative comparison of isolated drug−protein interactions in different lipid phases, but they are not simple thermodynamic parameters and contain multiple components. The thermodynamic justification for the use of ΔH^{rel}_{dp} and ΔS^{rel}_{dp} is presented in section S3 of the Supporting Information.

The free energy of transport activation ($\Delta G^{‡}$) was calculated using the absolute rate equation

$$\Delta G^{‡} = RT\left[\ln\left(\frac{K_b}{h}\right) - \ln\left(\frac{k_{app}}{T}\right)\right] \quad (4)$$

where K_b is Boltzmann's constant, h is Planck's constant, T is the temperature in kelvin, and R is the gas constant. Activation energies, and the entropic and enthalpic components at a given temperature, were calculated from the slope of log k_{app} versus $1/T$, using the following equations, as described previously.[39]

$$\frac{\partial(\ln k_{app})}{\partial\left(\frac{1}{T}\right)} = E_c/RT \quad (5)$$

$$k_{app} = Ae^{-(E_a/RT)} \quad (6)$$

$$\Delta H^{‡} = E_a - RT \quad (7)$$

$$T\Delta S^{‡} = \Delta H^{‡} - \Delta G^{‡} \quad (8)$$

RESULTS

Membrane Partitioning of the Drug Is Favored in Liquid-Crystalline Phase Lipid Bilayers. The extent of partitioning of the substrate into the membrane is important for their interaction with Pgp, because it essentially controls the effective concentration presented to the transporter. For example, the apparent affinities of *C. elegans* Pgp for binding paclitaxel and actinomycin D were increased 100- and 4000-fold, respectively, when the protein was in a membrane environment relative to detergent solution.[10] In our study, K_{lip} values were determined for LDS-751, H33342, and MK-571 in

dx.doi.org/10.1021/bi301532c | Biochemistry 2013, 52, 343−354

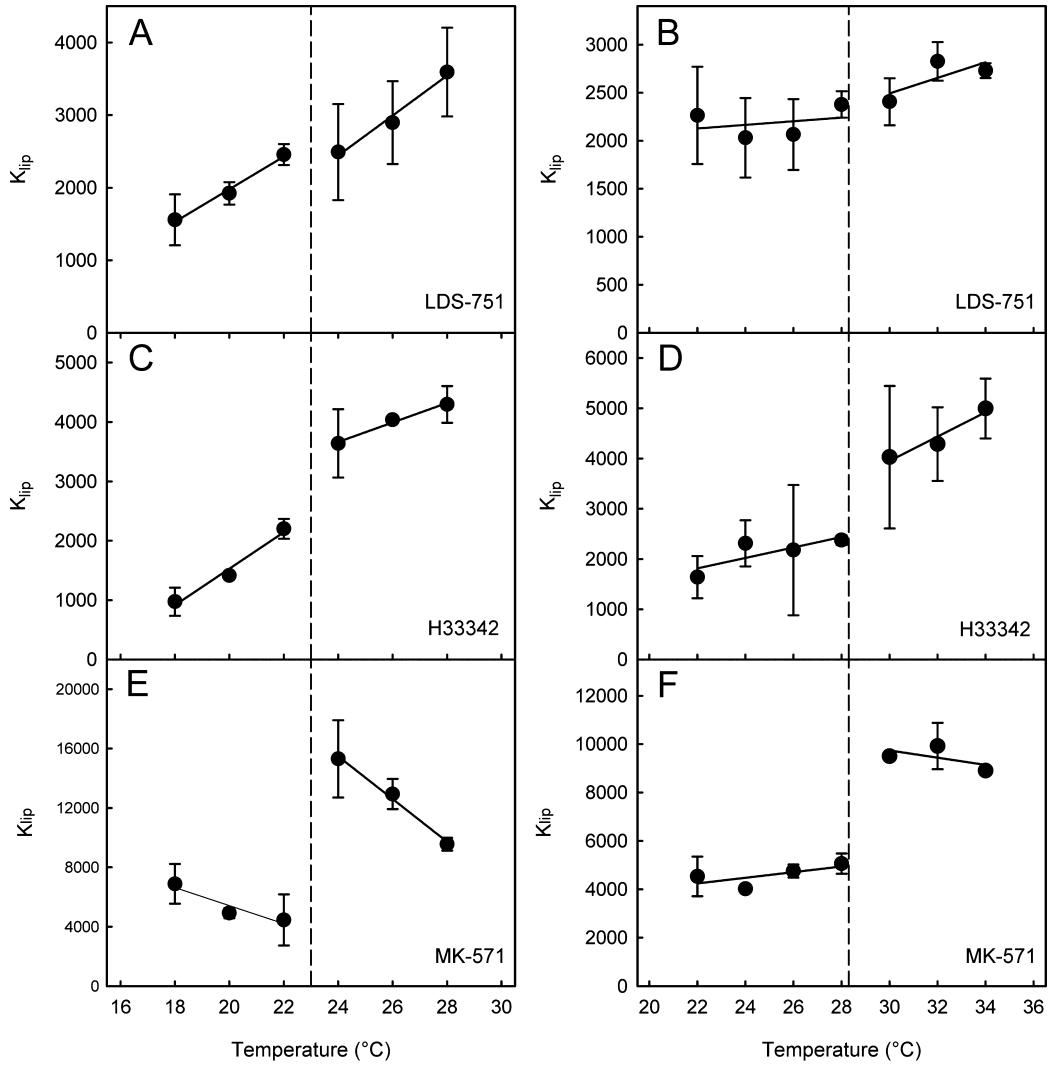

Figure 1. Effect of phospholipid bilayer melting on the lipid−water partition coefficients of Pgp substrates. K_{lip} values are presented as the means ± SD for LDS-751 (A and B), H33342 (C and D), and MK-571 (E and F) in DMPC bilayers (left) and PMPC bilayers (right). A vertical dashed line indicates the T_m for each phospholipid. Where not visible, error bars are included within the symbols.

DMPC or PMPC liposomes at several temperatures spanning the T_m values of the lipid bilayer. As shown in Figure 1, the values of K_{lip} for these drugs ranged from ∼1000 to 16000, and partitioning into liquid-crystalline phase lipid was always more favorable than that into gel phase lipid. The magnitude of the partition coefficient was dependent on drug structure, lipid phase, and lipid acyl chain length. Interestingly, the level of partitioning of MK-571 into DMPC bilayers decreased with an increasing temperature (within the same lipid phase), whereas the opposite was observed for the other two drugs.

Substrates Bind to Pgp with a Higher Affinity in Gel Phase Bilayers. Fluorescence-based approaches have proven to be very useful in quantifying the interactions of Pgp with its substrates.[40] Titration of Pgp proteoliposomes and detergent-solubilized Pgp with LDS-751, H33342, and MK-571 resulted in saturable quenching of Trp fluorescence as the drug concentration increased, which allowed the apparent binding affinity of Pgp for the drug (K_d) to be determined at different temperatures (Figure 2). For DMPC proteoliposomes (left panels), there was a clear discontinuity in both the value of K_d and the effect of temperature on K_d (slope of the line), above and below T_m. In comparison to DMPC, there was a smaller change in the K_d and slope as a result of the PMPC phase transition (right panels). The apparent binding affinity of Pgp for all three substrates was higher in gel phase than in liquid-crystalline phase DMPC and decreased as a result of the melting transition. In the case of PMPC, K_d showed essentially no change for LDS-751, and a modest change for H33342 and MK-571, as the bilayer melted. Overall, the apparent drug binding affinity of Pgp was often higher when the protein was reconstituted into bilayers of PMPC rather than DMPC, and always higher in the more rigid gel phase compared to the fluid liquid-crystalline phase.

Values of K_{dlip}, which represents the affinity of Pgp for drugs from within the membrane, were calculated as described in Materials and Methods, using the values of K_{lip} and K_d (Tables S1 and S2 of the Supporting Information). The calculated K_{dlip} values (Figure 3 and Tables S1 and S2 of the Supporting Information) show a discontinuity as a result of the phospholipid phase transition for both DMPC and PMPC. In DMPC proteoliposomes, the K_{dlip} values for binding of Pgp to LDS-751, H33342, and MK-571 ranged from 14 to 34 mM, from 11 to 53 mM, and from 31 to 71 mM, respectively, whereas in PMPC proteoliposomes, the affinities for LDS-751,

dx.doi.org/10.1021/bi301532c | *Biochemistry* 2013, 52, 343−354

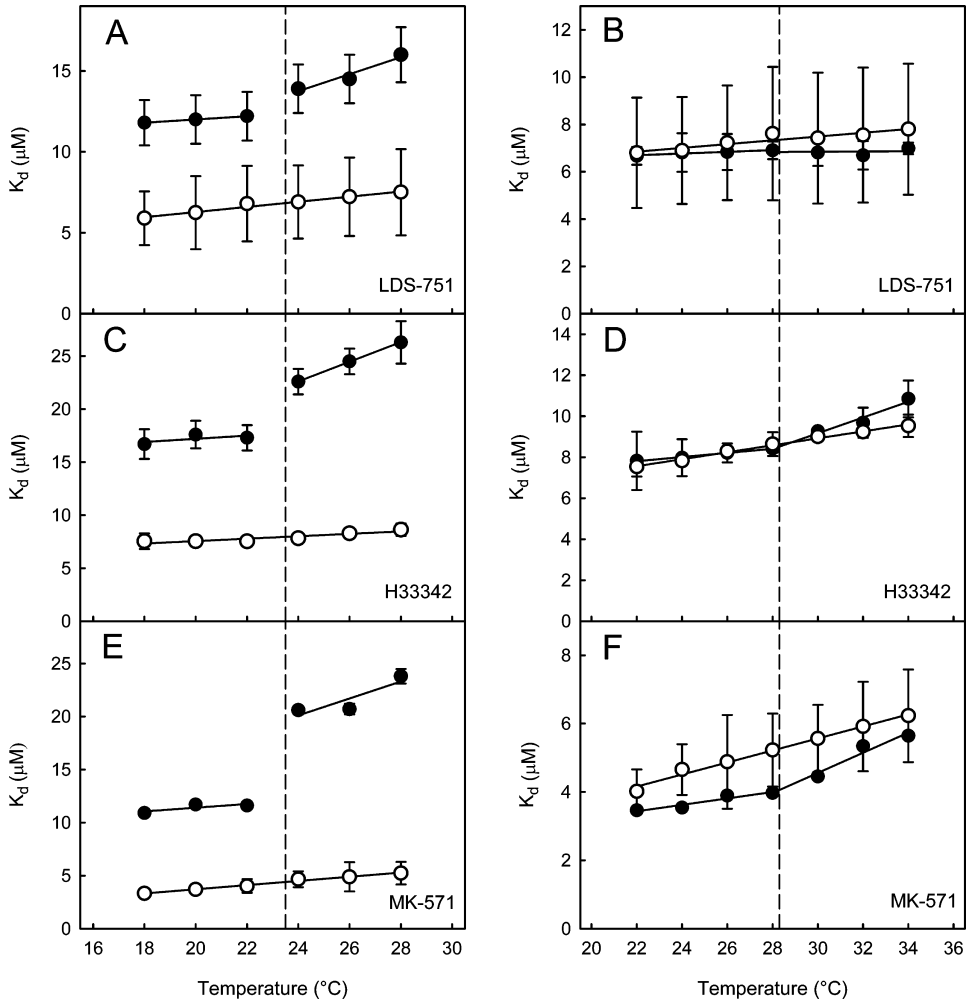

Figure 2. Effect of phospholipid bilayer melting on Pgp substrate binding affinity. K_d values are presented as the means ± SD obtained using Pgp proteoliposomes (●) or detergent-solubilized Pgp (○) for LDS-751 (A and B), H33342 (C and D), and MK-571 (E and F) in DMPC bilayers (left) and PMPC bilayers (right). A vertical dashed line indicates the T_m for each phospholipid. Where not visible, error bars are included within the symbols.

H33342, and MK-571 ranged from 12 to 14 mM, from 11 to 34 mM, and from 9 to 26 mM, respectively,. The affinity of Pgp for all three drugs is clearly increased in gel phase proteoliposomes, with the exception of LDS-751 in PMPC bilayers. Further, Pgp generally displayed higher affinity for a particular drug when reconstituted into PMPC proteoliposomes compared to DMPC proteoliposomes.

van't Hoff thermodynamic parameters were calculated for the lipid partitioning of drug (from K_{lip}) and for the binding of the drug to Pgp from the lipid phase (from K_{dlip}) and were found to vary for the different drugs and lipids used in these studies (Tables S3−S6 of the Supporting Information). In DMPC proteoliposomes, calculated free energies for binding of the drug to Pgp from the lipid phase ranged from −8.3 to −10.5 kJ/mol, from −7.5 to −10.8 kJ/mol, and from −6.6 to −8.8 kJ/mol for LDS-751, H33342, and MK-571, respectively. These values ranged from −11.3 to −11.7 kJ/mol, from −8.7 to −10.8 kJ/mol, and from −9.3 to −11.7 kJ/mol for LDS-751, H33342, and MK-571, respectively, in PMPC proteoliposomes. Formation of the drug−Pgp complex in the two different lipid bilayers was assessed using the parameters ΔH^{rel}_{dp} and ΔS^{rel}_{dp}, which eliminate the contribution of the lipid itself. In some cases, no change in these binding parameters was observed as a result of a change in the lipid environment (see Tables S7 and S8 of the Supporting Information). Notably, values of ΔH^{rel}_{dp} and ΔS^{rel}_{dp} (Table S7 of the Supporting Information) were both more favorable for MK-571 binding in gel phase PMPC than in liquid-crystalline phase PMPC.

Effect of the Lipid Bilayer on Drug Transport by Pgp.

To investigate the effect of lipid bilayer phase state on drug transport, a real-time fluorescence-based assay was used to determine H33342 and LDS-751 transport rates for Pgp reconstituted into proteoliposomes in different phase states. The assay for H33342 was reported previously,[17,41] and a similar approach was used to measure transport of LDS-751, which was established as a high-affinity Pgp substrate in earlier work.[42,43] Methodological improvements included the addition of membrane partitioning data, which allowed Pgp transport turnover numbers to be obtained for the first time in a reconstituted system. The apparent transport rates differed for the two drugs and the two host lipids used for reconstitution. Figure 4 shows the effect of temperature on the rate of drug transport for Pgp reconstituted into DMPC or PMPC. In the liquid-crystalline phase, the transport rates of H33342 were higher than those of LDS-751. For both drugs, there is a clear discontinuity in transport rates above and below T_m, with

dx.doi.org/10.1021/bi301532c | *Biochemistry* 2013, 52, 343−354

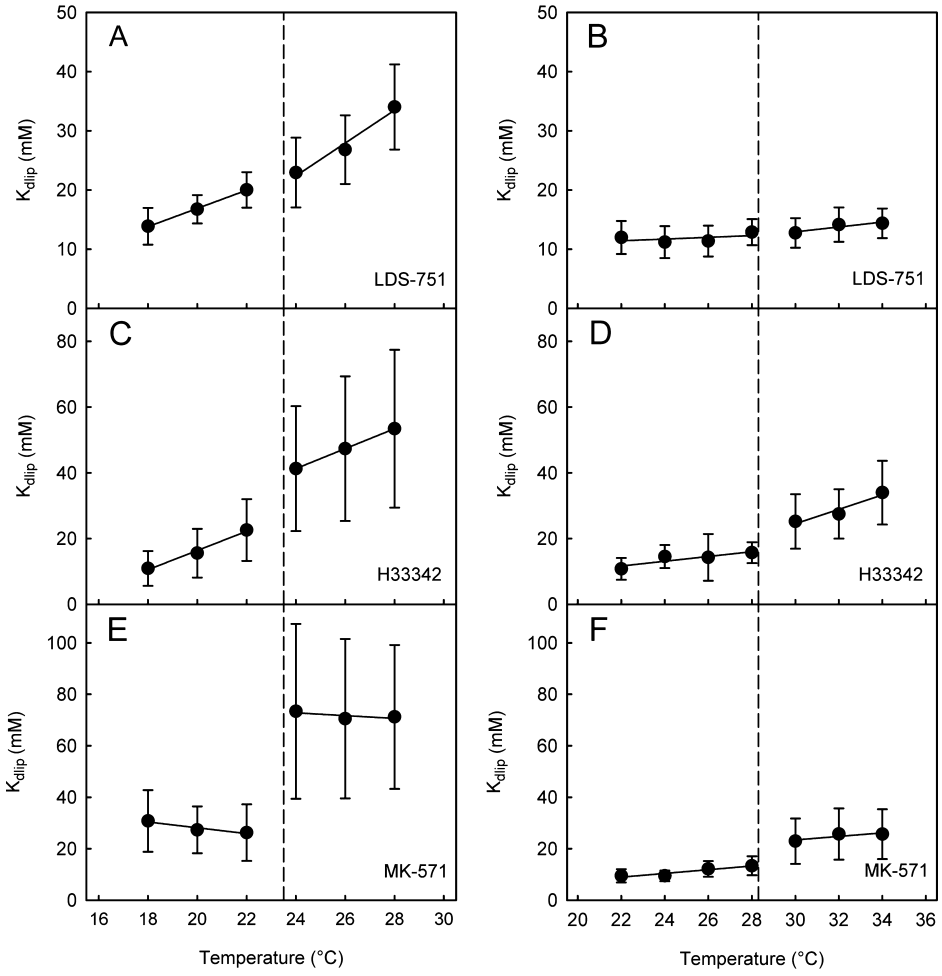

Figure 3. Effect of the gel to liquid-crystalline phase transition T_m on K_{dlip}. Data were calculated from the means of individual experiments, and errors were propagated from the SD for LDS-751 (A and B), H33342 (C and D), and MK-571 (E and F) in DMPC bilayers (left) and PMPC bilayers (right). A vertical dashed line indicates the T_m for each lipid.

higher transport rates observed in the liquid-crystalline phase in DMPC and PMPC. However, the magnitude of the change caused by lipid bilayer melting depends on both the drug and the lipid acyl chain length; larger changes were seen for H33342 than for LDS-751, and for PMPC than for DMPC.

Apparent turnover numbers, k_{app}, were obtained for drug transport at temperatures spanning T_m and used to calculate Arrhenius and transition state parameters for the different lipid phases. A representative set of values from this analysis is given in Table 1. The value of $\Delta G^{\ddagger}$ was relatively constant for all drugs in both lipids, with values ranging from 74.2 to 78.3 kJ/mol. A linear relationship between $\Delta S^{\ddagger}$ and $\Delta H^{\ddagger}$ was found for all drugs in gel phase bilayers at 22 °C (Figure 5A). Similarly, a linear relationship between $\Delta S^{\ddagger}$ and $\Delta H^{\ddagger}$ was observed for all drugs at 26 °C, regardless of whether lipids were in the gel or liquid-crystalline phase (Figure 5B). $\Delta H^{\ddagger}$ parameters were always positive, with values generally being higher in gel phase lipid.

For both LDS-751 and H33342 in DMPC and PMPC bilayers, the concentration dependence of the drug transport rates always showed a hyperbolic relationship [Michaelis–Menten-like (Figure 6A,C)] allowing the estimation of K_M and (taking into account drug–membrane partitioning) K_{Mlip}. Table 2 shows the effect of lipid phase state and acyl chain length on the K_M/K_{Mlip} of drug transport by reconstituted Pgp. It should be noted that K_M values are substantially lower (by approximately 3.9–11-fold) than K_d values obtained under the same conditions, and K_{Mlip} values are 3.8–9.7-fold lower than K_{dlip} values (Table 2 and Tables S1 and S2 of the Supporting Information). In contrast to drug transport, the effect of drug concentration on Pgp ATPase activity was either stimulatory or biphasic and did not fit a Michaelis–Menten-like relationship. Importantly, for LDS-751, an increase in ATPase activity at concentrations of >3 μM did not correspond to an increased transport rate (compare panels A and B of Figure 6), and H33342 transport appeared to approach saturation at concentrations substantially higher than those giving maximal ATPase activity (compare panels C and D of Figure 6).

DISCUSSION

The effect of the lipid phase and acyl chain length on the partitioning of three Pgp substrates into DMPC and PMPC bilayers was studied at temperatures spanning their T_m values. Measured values of K_{lip} fall within ranges previously determined for other Pgp substrates.[44,45] The results illustrate that drug partitioning is dependent on both drug chemical structure and membrane biophysical properties. LDS-751, H33342, and MK-571 all prefer to partition into liquid-crystalline lipid, a phenomenon previously observed for other lipophilic compounds.[14,15] Lipid bilayer melting results in a 4% increase in

dx.doi.org/10.1021/bi301532c | Biochemistry 2013, 52, 343–354

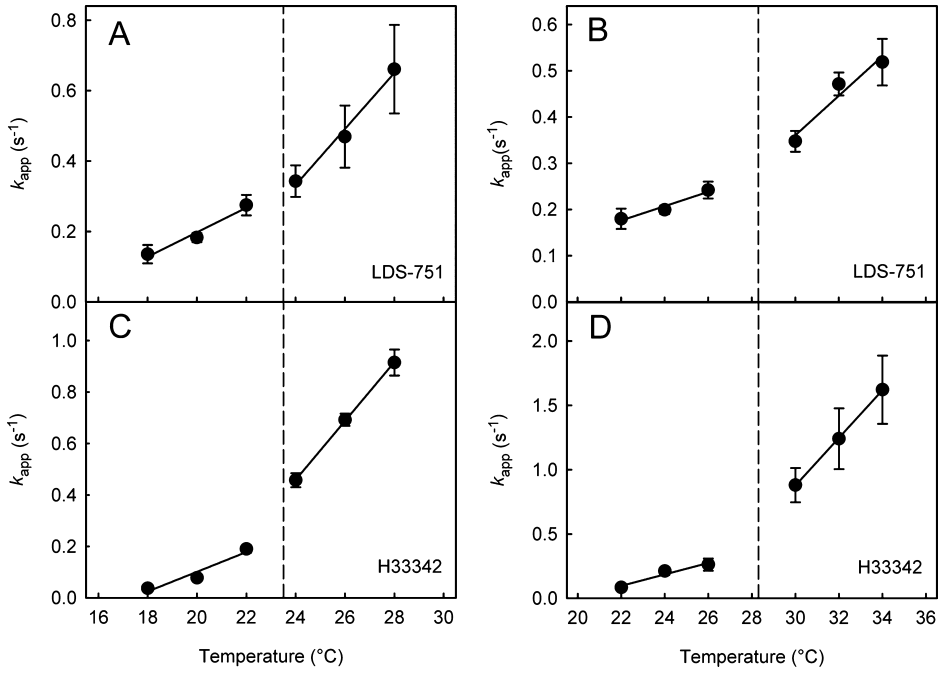

Figure 4. Effect of the gel to liquid-crystalline phase transition T_m on the transport of substrates by Pgp. Data are presented as the means ± SD for LDS-751 (A and B) and H33342 (C and D) in DMPC bilayers (left) and PMPC bilayers (right). A vertical dashed line indicates the T_m for each lipid. Where not visible, error bars are included within the symbols.

Table 1. Arrhenius and Transition State Thermodynamic Parameters for Drug Transport by Pgp[a]

lipid	drug	T (°C)	lipid phase[b]	k_{app} (s^{-1})	E_a (kJ/mol)	ln A (s^{-1})	$\Delta H^{\ddagger}$ (kJ/mol)	$T\Delta S^{\ddagger}$ (kJ/mol)	$\Delta G^{\ddagger}$ (kJ/mol)
DMPC	H33342	22	gel	0.19	293 ± 16	117 ± 7	291 ± 16	214 ± 16	76.4 ± 0.2
DMPC	LDS-751	22	gel	0.28	126 ± 12	50 ± 5	124 ± 12	48 ± 12	75.4 ± 0.3
DMPC	H33342	26	LC	0.69	129 ± 16	51 ± 6	127 ± 14	52 ± 14	74.2 ± 0.1
DMPC	LDS-751	26	LC	0.47	122 ± 4	48 ± 1	119 ± 4	44 ± 4	75.4 ± 0.3
PMPC	H33342	22	gel	0.09	208 ± 74	83 ± 30	206 ± 8	129 ± 8	78.3 ± 0.5
PMPC	LDS-751	22	gel	0.18	54 ± 16	20 ± 4	35 ± 16	−41 ± 16	76.1 ± 0.3
PMPC	H33342	30	LC	0.88	118 ± 74	47 ± 3	116 ± 74	41 ± 74	74.6 ± 0.4
PMPC	LDS-751	30	LC	0.37	78 ± 23	30 ± 9	61 ± 16	−16 ± 16	76.8 ± 0.2

[a]Conditions were as follows: pH 7.4, 5 mM ATP, and 5 μM H33342 or 4 μM LDS-751. Data were calculated as described in Materials and Methods from values obtained from at least two independent experiments, each performed in duplicate. Errors represent the error propagated through the calculation. [b]Gel, gel phase lipid; LC, liquid-crystalline phase lipid.

membrane volume,[46] so drugs likely partition better into a liquid-crystalline phase lipid because they fit more easily into the additional voids present in the membrane. Interestingly, the decrease in K_{lip} with an increasing temperature for MK-571 partitioning into DMPC suggests the existence of nonclassical hydrophobic interactions (i.e., a ΔH°-driven process); a similar effect was noted for an amphipathic lipopeptide.[47] This suggests that specific interactions between the drug and the lipid bilayer can contribute to drug−membrane partitioning. Regardless of the mechanism, small changes in acyl chain length or lipid phase state can drastically affect the membrane partitioning of substrates, which has functional implications for Pgp's ability to bind drugs within the bilayer and transport them to the aqueous phase.

When drug−membrane partitioning is taken into account, it was revealed that the affinity of Pgp for binding substrates within the bilayer (K_{dlip}) is in the range of 9−70 mM. These are the first estimates of the binding affinity of Pgp based on experimental measurement of both K_d and K_{lip}. On the basis of this relatively low intrinsic binding affinity, it seems likely that Pgp interacts weakly with its drug substrates, likely by van der Waals interactions and/or the hydrophobic effect. Chen and coworkers also suggested that *C. elegans* Pgp in membranes has a low intrinsic binding affinity for its substrates, based on the enhanced sensitivity of its ATPase activity to drug stimulation.[10] The crystal structure of mouse Pgp shows one or two cyclic peptide molecules interacting with the binding pocket via hydrophobic and aromatic amino acid side chains,[21] which supports this assertion. The relatively nonspecific nature of these interactions, coupled with the involvement of different amino acid side chains in binding different drugs, helps to explain the observation that Pgp interacts with such a large number of structurally diverse substrates. To the best of our knowledge, the only previous report of the affinity of Pgp for binding substrates in the lipid phase is that of Seelig and coworkers, who used indirect measurements of drug-stimulated ATPase activity to estimate K_{dlip} values that ranged from ∼0.5 to 4 mM for three Pgp substrates.[48] Given the differences in methodology and substrates, the K_{dlip} values in this study compare favorably. The free energy of partitioning of the drug from water to the lipid membrane was previously shown to account for a large proportion of the free energy of binding of

dx.doi.org/10.1021/bi301532c | *Biochemistry* 2013, 52, 343−354

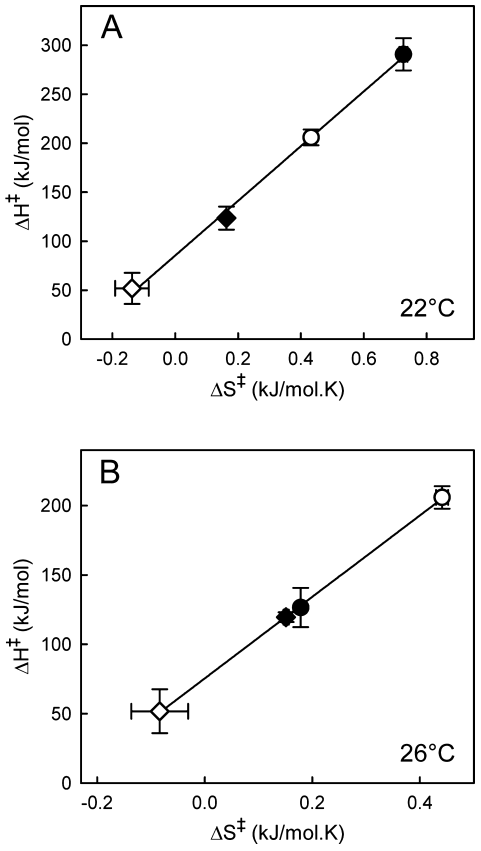

Figure 5. Isokinetic plots for the transport of LDS-751 and H33342 by Pgp. (A) Isokinetic plot for transport at 22 °C. Model parameters were as follows: r^2 = 0.9974, β = 5 ± 10 °C, $T_{S0}^{\ddagger}$ = −90 ± 7 kJ/mol, and $h_0^{\ddagger}$ = 85 ± 4 kJ/mol. (B) Isokinetic plot for transport at 26 °C. Model parameters were as follows: r^2 = 0.9997, β = 23 °C, $T_{S0}^{\ddagger}$ = −77 ± 1 kJ/mol, and $h_0^{\ddagger}$ = 76 ± 1 kJ/mol. LDS-751 in PMPC bilayers (◇), LDS-751 in DMPC bilayers (◆), H33342 in PMPC bilayers (○), and H33342 in DMPC bilayers (●). Error bars represent errors propagated through the calculation. Where not visible, error bars are included within the symbols.

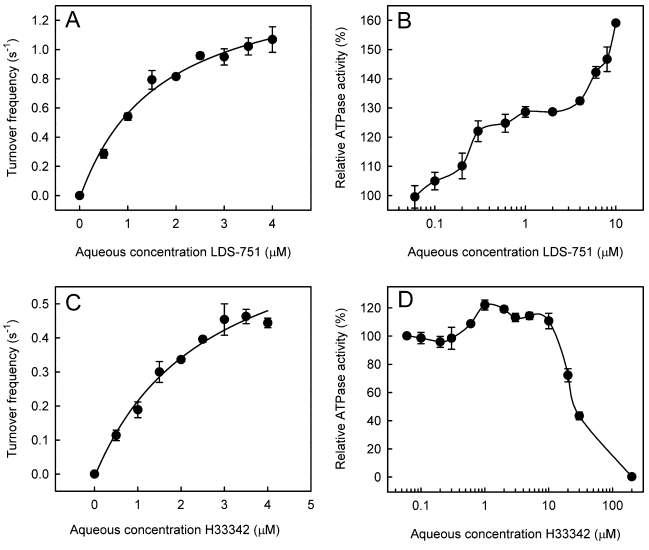

Figure 6. Dependence of transport rates and ATPase hydrolysis rates on the concentration of LDS-751 (A and B) and H33342 (C and D) for Pgp in PMPC bilayers. Experiments were conducted at 34 °C.

the drug to Pgp from the aqueous phase,[44] which is consistent with the studies presented here. For example, $\Delta G°$ for MK-571 binding from the aqueous phase to Pgp in DMPC bilayers (calculated from the K_d at 34 °C) is approximately −28 kJ/mol, compared to the $\Delta G°$ for partitioning (calculated from K_{lip}) of approximately −21 kJ/mol.

Our results showed that the affinity of Pgp for the substrate is higher in gel phase lipid than in liquid-crystalline phase lipid, and higher in PMPC than in DMPC (Figures 2 and 3 and Tables S1 and S2 of the Supporting Information). This is consistent with previous studies which reported that the drug binding to Pgp is tighter in a more rigid membrane environment.[14] Thermodynamic parameters derived from K_{dlip} values include both drug−lipid and drug−Pgp interactions, which complicates their interpretation. Changing the lipid environment (i.e., the host bilayer) clearly alters drug−lipid interactions (evident in K_{lip} values). Analysis of the thermodynamic parameters of binding and partitioning provided insight into how the overall interaction of Pgp and drug within the bilayer depends on both direct drug−protein interactions and drug−lipid interactions. Changes in the lipid-independent thermodynamics of formation of the drug−Pgp complex (assessed using ΔH_{dp}^{rel} and ΔS_{dp}^{rel}) were found to result from changes in both acyl chain length and lipid phase. For example, ΔH_{dp}^{rel} and ΔS_{dp}^{rel} were both more favorable for binding of MK-571 with PMPC in the gel phase compared to the liquid-crystalline phase (Table S7 of the Supporting Information), suggesting that, in this case, direct drug−Pgp interactions are more favorable in gel phase lipid. Changes in these interactions could be due to Pgp conformational changes in different host lipids (which could in turn affect the bilayer) or a change in the physical location of the drug molecules within the membrane. There are also several instances in which little difference was found in either ΔH_{dp}^{rel} or ΔS_{dp}^{rel} upon comparison of different lipid bilayers (Table S7 of the Supporting Information). In these cases, differences in K_{dlip} are likely caused by changes in drug−lipid interactions. Because the drug must leave the bilayer to bind to Pgp, a less favorable interaction between the drug and lipid (lower K_{lip}) would promote drug binding to the transporter. Thus, both drug−lipid and drug−Pgp interactions appear to contribute to the overall binding affinity and modulate changes in affinity observed with different lipid phases, acyl chain lengths, and drug types. It is likely that these complex interactions with lipids also contribute to the observed changes in transport rate.

The turnover numbers obtained in proteoliposomes for Pgp-mediated transport of LDS-751 and H33342 ranged from 0.04 to 1.6 s^{-1}, whereas previous estimates for vinblastine in cells were 1.1 s^{-1} at 25 °C and 1.4 s^{-1} at 37 °C.[49] Given the differences in substrates and lipid environments used in this work, these values compare favorably. Our experiments represent the first time that Pgp turnover numbers have been estimated in a purified reconstituted system. Importantly, the transport rates differ depending on the specific substrate used, which suggests that the catalytic transition state (likely a step in ATP hydrolysis) contains bound substrate, as previously proposed by al-Shawi et al.[39] In this study, transport rates for LDS-751 and H33342 were higher in liquid-crystalline bilayers than in the gel phase, in contrast to previous results for a tetramethylrosamine, a rhodamine dye.[15] This difference in behavior among the three substrates may be related to the temperature dependence of their partitioning into gel and liquid-crystalline lipid bilayers. As pointed out previously,[15] the

dx.doi.org/10.1021/bi301532c | Biochemistry 2013, 52, 343−354

Table 2. Kinetic Parameters for Drug Transport by Pgp Reconstituted into Lipid Bilayers of Different Phase States and Acyl Chain Lengths

		K_M (μM)		K_{Mlip} (mM)	
drug	lipid	gel phase[a]	LC phase[a]	gel phase[a]	LC phase[a]
LDS-751	DMPC	1.2 ± 0.3	1.5 ± 0.3	1.5 ± 0.5	3.5 ± 0.9
LDS-751	PMPC	0.8 ± 0.3	1.8 ± 0.1	1.4 ± 0.6	3.7 ± 0.7
H33342	DMPC	1.9 ± 0.4	2.8 ± 0.1	1.6 ± 0.5	7.4 ± 0.8
H33342	PMPC	1.4 ± 0.5	2.8 ± 0.1	1.9 ± 0.8	8.8 ± 2.4

[a]Temperatures were as follows: 18, 22, 28, and 34 °C for gel phase DMPC, gel phase PMPC, LC phase DMPC, and LC phase PMPC, respectively.

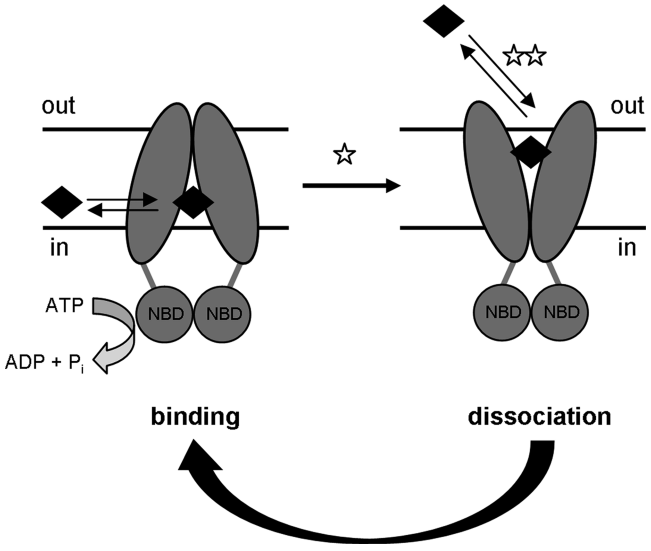

Figure 7. Simplified scheme for the transport of drug by Pgp. In the first step, the drug binds to Pgp in the inward-facing conformation, which couples ATP hydrolysis to drug transport. The hydrolysis of ATP causes a conformational change to the outward-facing conformation; this step contributes to the overall rate of drug transport (one star). In the outward-facing conformation, the bound drug molecule must dissociate to complete the transport cycle (two starts). To bind a new drug molecule to transport, Pgp must return to the inward-facing conformation, a step that might include the hydrolysis of ATP. If dissociation of the drug from the outward-facing conformation fails to occur, the result is an unsuccessful transport cycle. Thus, both the rate of drug dissociation and the rate of the inward−outward conformational change contribute to the net transport rate.

decrease in transport rate observed for tetramethylrosamine in liquid-crystalline phase DMPC and PMPC resembled the pattern seen for partitioning of *p*-alkylphenols into lipid bilayers,[50] which also declined with increasing temperature above T_m. In this study, LDS-751 and H33342 displayed the opposite behavior; their lipid−water partition coefficient increased with temperature in liquid-crystalline phase bilayers. However, as discussed below, the transport process involves multiple steps, and its rate is a complex function of several thermodynamic and kinetic parameters (not just partitioning); therefore, there is presently no clear-cut answer to this question. One proposed strategy for reducing the transport activity of Pgp involves modifying the fluidity of the lipid environment,[30] which may be ill-advised, given that the effect of lipid fluidity on transport appears to be drug-specific.

Although ATP hydrolysis clearly drives Pgp-mediated drug transport, the existence of high basal ATPase activity has made it difficult to address the energetic link between the two processes. The dependence of ATP hydrolysis rate on drug concentration clearly does not mirror the dependence of transport rate on drug concentration (Figure 6). Thus, the transport rate is not exclusively controlled by the ATP hydrolysis rate, supporting the suggestion of al-Shawi et al. that any single step in ATP turnover is unlikely to limit drug transport.[39] Further, this idea reconciles previous studies that showed increased ATPase activity,[16] but lower drug transport rates,[15] as a result of lipid bilayer melting.

The stoichiometry of ATP hydrolysis relative to drug transport for Pgp remains controversial. A near-stoichiometric ratio of ATP hydrolysis to drug molecules transported has been proposed[51,52] and is generally accepted, but values of 50 ATP molecules per transport cycle have also been reported.[53] The stoichiometry cannot be estimated on the basis of the relative rate constants for transport and ATPase activity, because the measured basal and drug-stimulated activities of Pgp cannot be easily separated. Further, if dissociation of drug limits the transport rate (see below), incomplete dissociation will result in a higher apparent ATP:transport stoichiometry. The values of $\Delta G^{\ddagger}$ for drug transport estimated here are very similar to the values of $\Delta G^{\ddagger}$ for ATP hydrolysis reported previously, which ranged from 67.6 to 75.2 kJ/mol.[39] The conditions used in the two studies are similar, so rough comparisons are possible. It appears that a single ATP molecule contains sufficient energy for the transport of one drug molecule. However, the approaches utilized here reveal only the highest-energy transition state; thus, it remains possible that an unidentified intermediate or lower-energy transition state might exist, requiring hydrolysis of a second ATP molecule to reprime Pgp. For this reason, it was not possible to estimate the stoichiometry of ATP hydrolysis relative to transported drug from the $\Delta G^{\ddagger}$ values. A transport cycle requiring hydrolysis of two ATP molecules for each drug molecule transported was previously proposed by Ambudkar and co-workers,[54] although this has not been confirmed by others and was later found not to apply to some Pgp mutants and substrates.[55]

In this work, the values of K_d (K_{dlip}) (Figures 2 and 3 and Tables S1 and S2 of the Supporting Information) were substantially higher than those of K_M (K_{Mlip}) (Table 2). If Pgp-mediated drug transport follows a typical Michaelis−Menten scheme

$$\mathrm{Pgp} + \mathrm{D_{in}} \underset{k_{-1}}{\overset{k_1}{\rightleftarrows}} \mathrm{Pgp{\cdot}D} \xrightarrow{k_2} \mathrm{Pgp} + \mathrm{D_{out}}$$

then

$$K_{Mlip}(K_M) = \frac{k_{-1} + k_2}{k_1} \quad (9)$$

$$K_{dlip}(K_d) = \frac{k_{-1}}{k_1} \quad (10)$$

dx.doi.org/10.1021/bi301532c | *Biochemistry* 2013, 52, 343−354

Because the value of K_{Mlip} must be greater than or equal to K_{dlip} in this scheme, it appears that Pgp transport cannot be described by a typical Michaelis−Menten scheme. However, if the second step (k_2) is considered to be reversible, i.e., drug dissociation is an equilibrium

$$\mathrm{Pgp} + \mathrm{D_{in}} \underset{k_{-1}}{\overset{k_1}{\rightleftarrows}} \mathrm{Pgp{\cdot}D} \underset{k_{-2}}{\overset{k_2}{\rightleftarrows}} \mathrm{Pgp} + \mathrm{D_{out}}$$

then

$$K_{Mlip}(K_M) = \frac{k_{-1} + k_2}{k_1 + k_{-2}} \tag{11}$$

$$K_{dlip}(K_d) = \frac{k_{-1}}{k_1} \tag{12}$$

In this scheme, if $k_{-2} > k_2$, then $K_{Mlip} < K_{dlip}$. Thus, it appears that the rate of dissociation of the drug from Pgp may contribute to the overall transport rate. This proposal is supported by the positive $\Delta S^{\ddagger}$ for LDS-751 and H33342 transport, which suggests that the process is limited by a dissociation event.[56] It is envisioned that the drug transport rate is partially controlled by the reappearance of the unoccupied drug binding site during the catalytic cycle, which is also consistent with a small K_{Mlip}/K_{dlip} ratio and the conclusions of others.[57]

One method of determining if the same transition state limits the rate of two processes is to verify the existence of a linear isokinetic plot ($\Delta H^{\ddagger}$ vs $\Delta S^{\ddagger}$ at a single temperature). Because $\Delta S^{\ddagger}$ and $\Delta H^{\ddagger}$ are derived from the same values, experimental errors can result in a linear isokinetic plot even if a common transition state does not exist. However, assuring that bidirectional error bars do not overlap is a simple test for verifying that linearity is not an experimental artifact.[58] It is clear from Figure 5 that a linear relationship between $\Delta S^{\ddagger}$ and $\Delta H^{\ddagger}$ exists for the transport of H33342 and LDS-751 in both gel and liquid-crystalline bilayers, implying that drug transport is limited by the same transition state regardless of the lipid environment. These results and those of al-Shawi[39] suggest that a single transition state controls the rate of Pgp drug transport.

Drug transport rates cannot be explained exclusively by the values of E_a or the pre-exponential factor A. There are several instances in Table 1 in which an increased transport rate is not accompanied by a decreased E_a. Therefore, different values of A must contribute to differences in transport rates. The value of A includes effects from the frequency of collisions between Pgp and drug, as well as molecular orientation effects. For the same drug and lipid phase, the value of A is generally lower in DMPC than in PMPC. There are also other clear instances in which the value of A changes with lipid phase. This could be a result of partitioning of the drug into different regions within the hydrophobic interior of DMPC or PMPC bilayers, or changes in Pgp conformation that affect its interaction with ATP or the drug. Regardless of the explanation, drugs appear to have different frequencies and/or orientations, with respect to their interactions with Pgp, in different lipid phases.

E_a is related to the magnitude of the conformational changes required to go from the ground state to the transition state. According to Eyring rate theory, processes with lower $\Delta H^{\ddagger}$ and $\Delta S^{\ddagger}$ values (closer to the bottom left corner of Figure 5) require fewer conformational changes to reach the transition state.[59] The lipid environment could contribute to the observed changes in transport by altering the number of rearrangements needed to reach the transition state. Drug transport by Pgp requires (at a minimum) the following steps: drug binding, hydrolysis of ATP, a conformational change, and drug dissociation. Drug transport rates do not appear to be limited exclusively by ATP hydrolysis. Results of these studies and those of al-Shawi[39,59] suggest that the rate of drug transport is modulated by the extent of conformational changes required to reach the transition state, and the affinity of the transition state for the drug. Taking this into account, we present a simple model for drug translocation in Figure 7. Changes in the transition state affinity for the drug would affect transport rates by modifying the chance of nonproductive decay of the transition state caused by the lack of drug dissociation.

■ ASSOCIATED CONTENT

Supporting Information

Details of calculations, thermodynamic analysis, and additional tables of data. This material is available free of charge via the Internet at http://pubs.acs.org.

■ AUTHOR INFORMATION

Corresponding Author

*Department of Molecular and Cellular Biology, Science Complex Room 2255, University of Guelph, Guelph, ON, Canada N1G 2W1. E-mail: fsharom@uoguelph.ca. Phone: (519) 824-4120, ext. 52247. Fax: (519) 837-1802.

Funding

This research was funded by the Canadian Cancer Society (Grant 700248).

Notes

The authors declare no competing financial interests.

■ ABBREVIATIONS

ABC, ATP-binding cassette; CHAPS, 3-[(3-cholamidopropyl)-dimethylammonio]-1-propanesulfonate; DMPC, 1,2-dimyristoylphosphatidylcholine; H33342, Hoechst 33342; LDS-751, 2-{4-[4-(dimethylamino)phenyl]-l,3-butadienyl}-3-ethylbenzothiazolium perchlorate; MDR, multidrug resistance/resistant; MK-571, 5-{3-[2-(7-chloroquinolin-2-yl)ethenyl]phenyl}-8-dimethylcarbamyl-4,6-dithiaoctanoic acid (sodium salt); NATA, *N*-acetyl-L-tryptophanamide; NBD, nucleotide binding domain; PC, phosphatidylcholine; Pgp, P-glycoprotein; PMPC, 1-palmitoyl-2-myristoylphosphatidylcholine; SD, standard deviation.

■ REFERENCES

(1) Dassa, E. (2011) Natural history of ABC systems: Not only transporters. *Essays Biochem. 50*, 19−42.

(2) Sharom, F. J. (2011) The P-glycoprotein multidrug transporter. *Essays Biochem. 50*, 161−178.

(3) Eckford, P. D., and Sharom, F. J. (2009) ABC efflux pump-based resistance to chemotherapy drugs. *Chem. Rev. 109*, 2989−3011.

(4) Sauna, Z. E., and Ambudkar, S. V. (2007) About a switch: How P-glycoprotein (ABCB1) harnesses the energy of ATP binding and hydrolysis to do mechanical work. *Mol. Cancer Ther. 6*, 13−23.

(5) Sharom, F. J. (2008) ABC multidrug transporters: Structure, function and role in chemoresistance. *Pharmacogenomics 9*, 105−127.

(6) Szakacs, G., Paterson, J. K., Ludwig, J. A., Booth-Genthe, C., and Gottesman, M. M. (2006) Targeting multidrug resistance in cancer. *Nat. Rev. Drug Discovery 5*, 219−234.

(7) Zolnerciks, J. K., Andress, E. J., Nicolaou, M., and Linton, K. J. (2011) Structure of ABC transporters. *Essays Biochem. 50*, 43−61.

(8) Romsicki, Y., and Sharom, F. J. (2001) Phospholipid flippase activity of the reconstituted P-glycoprotein multidrug transporter. *Biochemistry 40*, 6937−6947.
(9) Eckford, P. D., and Sharom, F. J. (2005) The reconstituted P-glycoprotein multidrug transporter is a flippase for glucosylceramide and other simple glycosphingolipids. *Biochem. J. 389*, 517−526.
(10) Jin, M. S., Oldham, M. L., Zhang, Q., and Chen, J. (2012) Crystal structure of the multidrug transporter P-glycoprotein from *Caenorhabditis elegans*. *Nature 490*, 566−569.
(11) Doige, C. A., Yu, X., and Sharom, F. J. (1993) The effects of lipids and detergents on ATPase-active P-glycoprotein. *Biochim. Biophys. Acta 1146*, 65−72.
(12) Urbatsch, I. L., and Senior, A. E. (1995) Effects of lipids on ATPase activity of purified Chinese hamster P-glycoprotein. *Arch. Biochem. Biophys. 316*, 135−140.
(13) Li-Blatter, X., Nervi, P., and Seelig, A. (2009) Detergents as intrinsic P-glycoprotein substrates and inhibitors. *Biochim. Biophys. Acta 1788*, 2335−2344.
(14) Romsicki, Y., and Sharom, F. J. (1999) The membrane lipid environment modulates drug interactions with the P-glycoprotein multidrug transporter. *Biochemistry 38*, 6887−6896.
(15) Lu, P., Liu, R., and Sharom, F. J. (2001) Drug transport by reconstituted P-glycoprotein in proteoliposomes. Effect of substrates and modulators, and dependence on bilayer phase state. *Eur. J. Biochem. 268*, 1687−1697.
(16) Romsicki, Y., and Sharom, F. J. (1998) The ATPase and ATP-binding functions of P-glycoprotein-modulation by interaction with defined phospholipids. *Eur. J. Biochem. 256*, 170−178.
(17) Eckford, P. D., and Sharom, F. J. (2008) Interaction of the P-glycoprotein multidrug efflux pump with cholesterol: Effects on ATPase activity, drug binding and transport. *Biochemistry 47*, 13686−13698.
(18) Aanismaa, P., Gatlik-Landwojtowicz, E., and Seelig, A. (2008) P-glycoprotein senses its substrates and the lateral membrane packing density: Consequences for the catalytic cycle. *Biochemistry 47*, 10197−10207.
(19) Callaghan, R., Ford, R. C., and Kerr, I. D. (2006) The translocation mechanism of P-glycoprotein. *FEBS Lett. 580*, 1056−1063.
(20) al-Shawi, M. K. (2011) Catalytic and transport cycles of ABC exporters. *Essays Biochem. 50*, 63−83.
(21) Aller, S. G., Yu, J., Ward, A., Weng, Y., Chittaboina, S., Zhuo, R., Harrell, P. M., Trinh, Y. T., Zhang, Q., Urbatsch, I. L., and Chang, G. (2009) Structure of P-glycoprotein reveals a molecular basis for poly-specific drug binding. *Science 323*, 1718−1722.
(22) Gutmann, D. A., Ward, A., Urbatsch, I. L., Chang, G., and Van Veen, H. W. (2010) Understanding polyspecificity of multidrug ABC transporters: Closing in on the gaps in ABCB1. *Trends Biochem. Sci. 35*, 36−42.
(23) Verhalen, B., Ernst, S., Borsch, M., and Wilkens, S. (2012) Dynamic ligand-induced conformational rearrangements in P-glycoprotein as probed by fluorescence resonance energy transfer spectroscopy. *J. Biol. Chem. 287*, 1112−1127.
(24) Robert, J., and Jarry, C. (2003) Multidrug resistance reversal agents. *J. Med. Chem. 46*, 4805−4817.
(25) Palmeira, A., Sousa, E., Vasconcelos, M. H., and Pinto, M. M. (2012) Three decades of P-gp inhibitors: Skimming through several generations and scaffolds. *Curr. Med. Chem. 19*, 1946−2025.
(26) Sinicrope, F. A., Dudeja, P. K., Bissonnette, B. M., Safa, A. R., and Brasitus, T. A. (1992) Modulation of P-glycoprotein-mediated drug transport by alterations in lipid fluidity of rat liver canalicular membrane vesicles. *J. Biol. Chem. 267*, 24995−25002.
(27) Callaghan, R., Stafford, A., and Epand, R. M. (1993) Increased accumulation of drugs in a multidrug resistant cell line by alteration of membrane biophysical properties. *Biochim. Biophys. Acta 1175*, 277−282.
(28) Woodcock, D. M., Linsenmeyer, M. E., Chojnowski, G., Kriegler, A. B., Nink, V., Webster, L. K., and Sawyer, W. H. (1992) Reversal of multidrug resistance by surfactants. *Br. J. Cancer 66*, 62−68.
(29) Drori, S., Eytan, G. D., and Assaraf, Y. G. (1995) Potentiation of anticancer-drug cytotoxicity by multidrug-resistance chemosensitizers involves alterations in membrane fluidity leading to increased membrane permeability. *Eur. J. Biochem. 228*, 1020−1029.
(30) Regev, R., Assaraf, Y. G., and Eytan, G. D. (1999) Membrane fluidization by ether, other anesthetics, and certain agents abolishes P-glycoprotein ATPase activity and modulates efflux from multidrug-resistant cells. *Eur. J. Biochem. 259*, 18−24.
(31) Doige, C. A., and Sharom, F. J. (1991) Strategies for the purification of P-glycoprotein from multidrug-resistant Chinese hamster ovary cells. *Protein Expression Purif. 2*, 256−265.
(32) Liu, R., Siemiarczuk, A., and Sharom, F. J. (2000) Intrinsic fluorescence of the P-glycoprotein multidrug transporter: Sensitivity of tryptophan residues to binding of drugs and nucleotides. *Biochemistry 39*, 14927−14938.
(33) Chifflet, S., Torriglia, A., Chiesa, R., and Tolosa, S. (1988) A method for the determination of inorganic phosphate in the presence of labile organic phosphate and high concentrations of protein: Application to lens ATPases. *Anal. Biochem. 168*, 1−4.
(34) Bradford, M. M. (1976) A rapid and sensitive method for the quantitation of microgram quantities of protein utilizing the principle of protein-dye binding. *Anal. Biochem. 72*, 248−254.
(35) Ebel, H., Grabitz, P., and Heimburg, T. (2001) Enthalpy and volume changes in lipid membranes. I. The proportionality of heat and volume changes in the lipid melting transition and its implication for the elastic constants. *J. Phys. Chem. B 105*, 7353−7360.
(36) Romsicki, Y., and Sharom, F. J. (1997) Interaction of P-glycoprotein with defined phospholipid bilayers: A differential scanning calorimetric study. *Biochemistry 36*, 9807−9815.
(37) Pauletti, G. M., and Wunderli-Allenspach, H. (1994) Partition coefficients in vitro: Artificial membranes as a standardized distribution model. *Eur. J. Pharm. Sci. 1*, 273−282.
(38) Parry, G., Palmer, D. N., and Williams, D. J. (1976) Ligand partitioning into membranes: Its significance in determining K_m and K_s values for cytochrome P-450 and other membrane bound receptors and enzymes. *FEBS Lett. 67*, 123−129.
(39) al-Shawi, M. K., Polar, M. K., Omote, H., and Figler, R. A. (2003) Transition state analysis of the coupling of drug transport to ATP hydrolysis by P-glycoprotein. *J. Biol. Chem. 278*, 52629−52640.
(40) Sharom, F. J., Liu, R., Qu, Q., and Romsicki, Y. (2001) Exploring the structure and function of the P-glycoprotein multidrug transporter using fluorescence spectroscopic tools. *Semin. Cell Dev. Biol. 12*, 257−265.
(41) Eckford, P. D., and Sharom, F. J. (2006) P-glycoprotein (ABCB1) interacts directly with lipid-based anti-cancer drugs and platelet-activating factors. *Biochem. Cell Biol. 84*, 1022−1033.
(42) Lugo, M. R., and Sharom, F. J. (2005) Interaction of LDS-751 with P-glycoprotein and mapping of the location of the R drug binding site. *Biochemistry 44*, 643−655.
(43) Lugo, M. R., and Sharom, F. J. (2009) Interaction of LDS-751 with the drug-binding site of P-glycoprotein: A Trp fluorescence steady-state and lifetime study. *Arch. Biochem. Biophys. 492*, 17−28.
(44) Gatlik-Landwojtowicz, E., Aanismaa, P., and Seelig, A. (2006) Quantification and characterization of P-glycoprotein-substrate interactions. *Biochemistry 45*, 3020−3032.
(45) Seelig, J., and Ganz, P. (1991) Nonclassical hydrophobic effect in membrane binding equilibria. *Biochemistry 30*, 9354−9359.
(46) Heimburg, T. (1998) Mechanical aspects of membrane thermodynamics. Estimation of the mechanical properties of lipid membranes close to the chain melting transition from calorimetry. *Biochim. Biophys. Acta 1415*, 147−162.
(47) Gorfe, A. A., Baron, R., and McCammon, J. A. (2008) Water-membrane partition thermodynamics of an amphiphilic lipopeptide: An enthalpy-driven hydrophobic effect. *Biophys. J. 95*, 3269−3277.
(48) Meier, M., Blatter, X. L., Seelig, A., and Seelig, J. (2006) Interaction of verapamil with lipid membranes and P-glycoprotein: Connecting thermodynamics and membrane structure with functional activity. *Biophys. J. 91*, 2943−2955.

(49) Ambudkar, S. V., Cardarelli, C. O., Pashinsky, I., and Stein, W. D. (1997) Relation between the turnover number for vinblastine transport and for vinblastine-stimulated ATP hydrolysis by human P-glycoprotein. *J. Biol. Chem. 272*, 21160−21166.
(50) Rogers, J. A., and Davis, S. S. (1980) Functional group contributions to the partitioning of phenols between liposomes and water. *Biochim. Biophys. Acta 598*, 392−404.
(51) Eytan, G. D., Regev, R., and Assaraf, Y. G. (1996) Functional reconstitution of P-glycoprotein reveals an apparent near stoichiometric drug transport to ATP hydrolysis. *J. Biol. Chem. 271*, 3172−3178.
(52) Shapiro, A. B., and Ling, V. (1998) Stoichiometry of coupling of rhodamine 123 transport to ATP hydrolysis by P-glycoprotein. *Eur. J. Biochem. 254*, 189−193.
(53) Shapiro, A. B., and Ling, V. (1994) ATPase activity of purified and reconstituted P-glycoprotein from Chinese hamster ovary cells. *J. Biol. Chem. 269*, 3745−3754.
(54) Sauna, Z. E., and Ambudkar, S. V. (2000) Evidence for a requirement for ATP hydrolysis at two distinct steps during a single turnover of the catalytic cycle of human P-glycoprotein. *Proc. Natl. Acad. Sci. U.S.A. 97*, 2515−2520.
(55) Maki, N., Moitra, K., Ghosh, P., and Dey, S. (2006) Allosteric modulation bypasses the requirement for ATP hydrolysis in regenerating low affinity transition state conformation of human P-glycoprotein. *J. Biol. Chem. 281*, 10769−10777.
(56) Pixton, D. A., Petersen, C. A., Franke, A., van, E. R., Garton, E. M., and Andrew, C. R. (2009) Activation parameters for heme-NO binding in *Alcaligenes xylosoxidans* cytochrome c′: The putative dinitrosyl intermediate forms via a dissociative mechanism. *J. Am. Chem. Soc. 131*, 4846−4853.
(57) Li-Blatter, X., Beck, A., and Seelig, A. (2012) P-Glycoprotein-ATPase modulation: The molecular mechanisms. *Biophys. J. 102*, 1383−1393.
(58) Liu, L., and Guo, Q. X. (2001) Isokinetic relationship, isoequilibrium relationship, and enthalpy-entropy compensation. *Chem. Rev. 101*, 673−695.
(59) Omote, H., Figler, R. A., Polar, M. K., and al-Shawi, M. K. (2004) Improved energy coupling of human P-glycoprotein by the glycine 185 to valine mutation. *Biochemistry 43*, 3917−3928.